

# Superconductivity, nematicity, and charge density wave in high- $T_c$ cuprates: A common thread

Zhong-Bing Huang,<sup>1,2,\*</sup> Shi-Chao Fang,<sup>1</sup> and Hai-Qing Lin<sup>2</sup>

<sup>1</sup>Faculty of Physics and Electronic Technology, Hubei University, Wuhan 430062, China

<sup>2</sup>Beijing Computational Science Research Center, Beijing 100193, China

(Dated: September 14, 2021)

To address the issues of superconducting and charge properties in high- $T_c$  cuprates, we perform a quantum Monte Carlo study of an extended three-band Emery model, which explicitly includes attractive interaction  $V_{OO}$  between oxygen orbitals. In the physically relevant parameter range, we find that  $V_{OO}$  acts to strongly enhance the long-range part of d-wave pairing correlation, with a clear tendency to form long-range superconducting order in the thermodynamic limit. Simultaneously, increasing  $|V_{OO}|$  renders a rapid increase of the nematic charge structure factor at most of wavevectors, especially near  $\mathbf{q} = (0, 0)$ , indicating a dramatic enhancement of nematicity and charge density waves. Our findings suggest that the attraction between oxygen orbitals in high- $T_c$  cuprates is a common thread linking their superconducting and charge properties.

*Introduction*— Superconductivity (SC) and mysterious pseudogap in high- $T_c$  cuprates have been the challenging issues in the condensed matter physics community [1–8]. The pseudogap phase setting in at the temperature  $T^*$  harbours a rich variety of symmetry-broken orders [1]. Nematicity, a  $C_4$  rotational-symmetry-broken order, is manifested by different in-plane anisotropic properties [9–14] below the onset temperature  $T_{nem}$ . The coincidence of  $T_{nem}$  and  $T^*$  observed in some experiments including transport measurement [13] and scanning tunneling microscope [14] strongly suggests that nematicity has an intimate relation to the formation of pseudogap. Another emerging order, the so-called charge density wave (CDW), prevalent in all chemically distinct families of cuprates, simultaneously breaks the rotational and translational symmetries [15–19]. This order sets in between 100 K and 200 K and has a d-wave form factor between  $O_x$  and  $O_y$  orbitals on the  $\text{CuO}_2$  plane [20, 21].

Recently, Raman scattering spectroscopies of several copper oxides showed that with decreasing the hole doping density, the pseudogap energy scale increases in a similar manner to the doping dependence of the CDW and antinodal superconducting energy scales. In addition, the latter two have almost equal values over a substantial doping region. These observations revealed that the three energy scales may be governed by a common thread, and the CDW and d-wave SC are intimately related [22, 23].

Tremendous theoretical attempts have been made to understand the d-wave SC, nematicity and CDW in high- $T_c$  cuprates based on the single- and multi-band models, but so far the answers remain highly controversial. First, both positive [24–35] and negative [36–42] evidence was found for the existence of d-wave SC, depending on the computational methods, all of which have their pros and cons. Second, although nematicity could be induced either by a d-wave Pomeranchuk instability [43, 44] or via quantum melting of charge stripes [45, 46], its stability is limited at temperatures about one order of magnitude lower than  $T_{nem}$  and/or in a narrow filling region near the van Hove singularity [43, 44, 47]. Moreover, it remains controversial on the main contribution to the formation of nematicity and CDW, with possible candidates including the off-site Coulomb repulsion between oxygen sites [48, 49], the

on-site Coulomb repulsion at the copper site [50], and spin fluctuations [51, 52]. Given the robustness of d-wave SC, nematicity and CDW in high- $T_c$  cuprates, divergent theoretical conclusions suggest that a key ingredient may be missing in the microscopic models.

In this Letter, we study the superconducting and charge properties in the realistic three-band Emery model [53] extended by an effective attraction  $V_{OO}$  between oxygen orbitals. The introduction of  $V_{OO}$  is justified by a recent angle-resolved photoemission experiment [54] on the one-dimensional cuprate  $\text{Ba}_{2-x}\text{Sr}_x\text{CuO}_{3+\delta}$  across a wide range of hole doping, showing an anomalously strong holon folding branch near  $k_F$ . A comparison with the theory reveals there exists a strong nearest-neighbor (NN) attraction of the order of  $eV$  in the studied compound. Due to structural and chemical similarities among cuprates, such a NN attraction may also be applicable to the 2D high- $T_c$  cuprates. Physically,  $V_{OO}$  can arise from coupling to certain bosonic excitations, such as quantized waves of electronic polarization [55] and phonons [56–58].

Our main results were obtained by the constrained-path Monte Carlo (CPMC) method [59–61], which can precisely capture the ground-state information of correlated electron systems. As expected, since attractive  $V_{OO}$  favors the hole pairing between oxygen orbitals, it induces a strong enhancement of the long-range part of d-wave pairing correlation. Unexpectedly,  $V_{OO}$  gives rise to an enhancement of the nematic charge structure factor at most of wavevectors, and the enhancement effect is particularly strong near  $\mathbf{q} = (0, 0)$ . This indicates that  $V_{OO}$  benefits the formation of  $\mathbf{q} = (0, 0)$  nematicity and finite  $\mathbf{q}$  CDW. Our findings demonstrate that the attraction between oxygen orbitals is crucial for a universal understanding of d-wave SC, nematicity and CDW in high- $T_c$  cuprates.

*Model and computational method*— To understand the physics of  $\text{CuO}_2$  plane, we adopt the following Hamiltonian,

$$H = H_{Emery} + H_{attract}, \quad (1)$$

where  $H_{Emery}$  and  $H_{attract}$  stand for the standard three-band Emery model [53] and attractive interaction between oxygen

orbitals, respectively. They are expressed in the form:

$$H_{Emery} = \sum_{\langle i,j \rangle \sigma} t_{pd}^{ij} (d_{i\sigma}^\dagger p_{j\sigma} + h.c.) + \epsilon \sum_{j\sigma} n_{j\sigma}^p + \sum_{\langle j,k \rangle \sigma} t_{pp}^{jk} (p_{j\sigma}^\dagger p_{k\sigma} + h.c.) + U_d \sum_i n_{i\uparrow}^d n_{i\downarrow}^d, \quad (2)$$

$$H_{attract} = V_{OO} \sum_{\langle\langle j,k \rangle\rangle} n_j^p n_k^p, \quad (3)$$

Here,  $d_{i\sigma}^\dagger$  is the creation operator of a Cu  $3d_{x^2-y^2}$  hole and  $p_{j\sigma}^\dagger$  is the creation operator of an O  $2p_x$  or  $2p_y$  hole.  $t_{pd}^{ij} = \pm t_{pd}$  and  $t_{pp}^{jk} = \pm t_{pp}$  are the NN Cu-O and O-O hybridizations, respectively, with the Cu and O orbital phase factors included in the sign.  $U_d$  and  $\epsilon$  denote the Coulomb repulsion at the Cu site and the charge-transfer energy.  $V_{OO}$  stands for attraction between O sites separated by a Cu site, and the corresponding summation restriction is denoted by  $\langle\langle j, k \rangle\rangle$ . In units of  $t_{pd}$ , we choose a physically relevant parameter set  $U_d = 6.0$ ,  $\epsilon = 3.0$ , and  $t_{pp} = 0.5$ , while  $V_{OO}$  is varied from 0.0 to  $-0.6$ .

Our calculations were performed on the square lattices of  $N = L \times L$  unit cells with periodic boundary conditions imposed using the CPMC method [59–61]. The basic strategy of CPMC is to project out the ground-state wave function from an initial wave function by branching random walk in an overcomplete space of constrained Slater determinants, which have positive overlaps with a known trial wave function. In this work, we focus on the closed-shell case, for which the corresponding free-electron wave function is non-degenerate and translationally invariant. In this case, the free-electron wave function is a good choice as the trial wave function [60, 62, 63].

The d-wave pairing correlation is defined as:

$$C(\mathbf{R}) = \langle \Delta_d^\dagger(\mathbf{R}) \Delta_d(\mathbf{0}) \rangle, \quad (4)$$

where

$$\Delta_d(\mathbf{R}) = \sum_{\mu} f_d(\mu) \{ [d_{\mathbf{R}\uparrow} d_{\mathbf{R}+\mu\downarrow} - d_{\mathbf{R}\downarrow} d_{\mathbf{R}+\mu\uparrow}] + [p_{\mathbf{R}\uparrow}^x p_{\mathbf{R}+\mu\downarrow}^x - p_{\mathbf{R}\downarrow}^x p_{\mathbf{R}+\mu\uparrow}^x] + [p_{\mathbf{R}\uparrow}^y p_{\mathbf{R}+\mu\downarrow}^y - p_{\mathbf{R}\downarrow}^y p_{\mathbf{R}+\mu\uparrow}^y] \}$$

with  $\mu = \pm \hat{x}, \pm \hat{y}$ . The d-wave form factor  $f_d(\mu) = 1$  for  $\mu = \pm \hat{x}$  and  $f_d(\mu) = -1$  for  $\mu = \pm \hat{y}$ . The vertex contribution to the pairing correlation is given by,

$$V(\mathbf{R}) = C(\mathbf{R}) - C'(\mathbf{R}), \quad (5)$$

where  $C'(\mathbf{R})$  is the bubble contribution from the dressed (interacting) propagator [64]. For convenience, we also define the partial averages of pairing correlation and its vertex contribution:  $\bar{C}(R > 2.0) = (1/N') \sum_{R > 2.0} C(\mathbf{R})$  and  $\bar{V}(R > 2.0) = (1/N') \sum_{R > 2.0} V(\mathbf{R})$ , where  $N'$  is the number of hole pairs with  $R > 2.0$ .

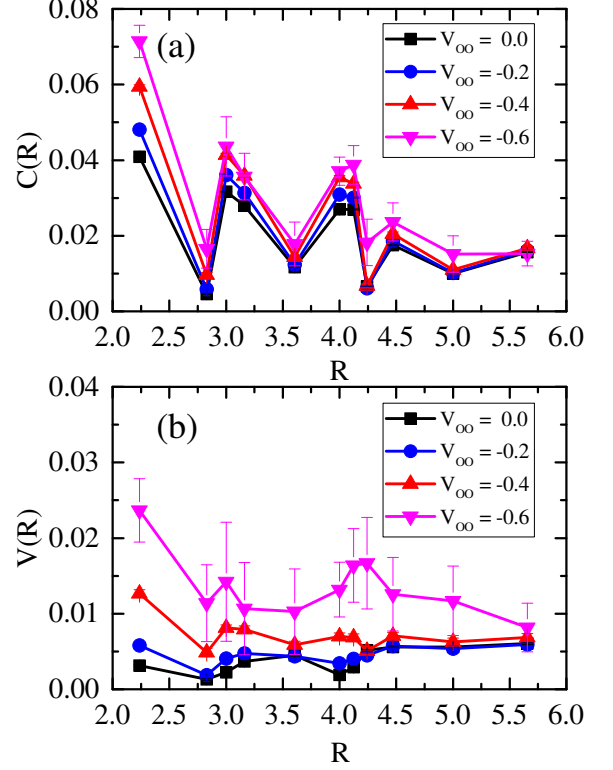


FIG. 1. (color online) (a) D-wave pairing correlation  $C(R)$  and (b) vertex contribution  $V(R)$  as a function of the distance  $R$  on the  $8 \times 8$  lattice at a hole doping density  $\delta = 0.156$ . The value of  $V_{OO}$  is indicated by the shape of symbol.

To understand the charge property, we compute the nematic charge correlation  $N^d(\mathbf{R})$  and corresponding structure factor  $N^d(\mathbf{q})$ , which are defined as,

$$N^d(\mathbf{R}) = \langle (n_{\mathbf{R}}^{px} - n_{\mathbf{R}}^{py})(n_{\mathbf{0}}^{px} - n_{\mathbf{0}}^{py}) \rangle, \quad (6)$$

$$N^d(\mathbf{q}) = \sum_{\mathbf{R}} e^{i\mathbf{q}\cdot\mathbf{R}} N^d(\mathbf{R}). \quad (7)$$

Here, the minus sign in Eq. (6) reflects the d-wave form factor or  $\pi$ -phase difference of charge distribution between  $O_x$  and  $O_y$  orbitals.

*Superconducting property*– In Figs. 1(a) and 1(b) we show  $C(R)$  and  $V(R)$  as a function of  $R$  and  $V_{OO}$  on the  $8 \times 8$  lattice at a hole doping density  $\delta = 0.156$ . At  $V_{OO} = 0.0$ , both  $C(R)$  and  $V(R)$  take small positive values, which are consistent with previous results on the  $6 \times 4$  [62] and  $6 \times 6$  [63] lattices. With decreasing  $V_{OO}$  from 0.0 to  $-0.6$ , one can clearly see that both pairing correlation and its vertex contribution monotonically increase at all long-range distances for  $R > 2.0$ . Our simulations demonstrate that the attractive interaction between oxygen orbitals is favorable for the d-wave SC. This is in sharp contrast to the situation of one-band  $t-U-V$  Hubbard model, where a NN attractive  $V$  was expected to enhance the d-wave

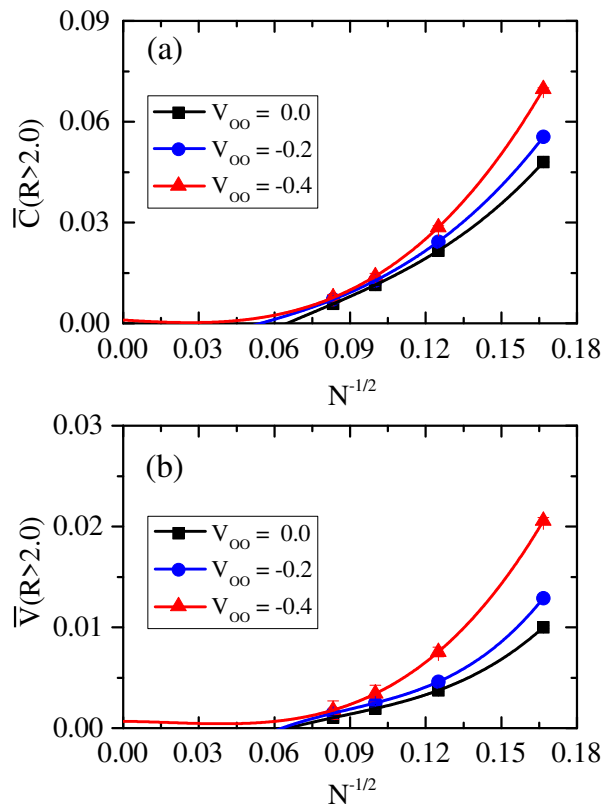


FIG. 2. (color online) (a) Partial average of pairing correlation  $\bar{C}(R > 2.0)$  and (b) partial average of vertex contribution  $\bar{V}(R > 2.0)$  as a function of  $1/\sqrt{N}$  for different values of  $V_{OO}$ . The data for a fixed  $V_{OO}$  are fitted by using third order polynomials in  $1/\sqrt{N}$ .

SC [65], however, numerical studies indicated that the d-wave pairing correlation can hardly be enhanced by  $V$  [66, 67].

To determine whether the d-wave SC exists in the extended three-band Emery model, we examine the evolution of pairing correlation and its vertex contribution with the lattice size. In Fig. 2 we plot  $\bar{C}(R > 2.0)$  and  $\bar{V}(R > 2.0)$  as a function of  $1/\sqrt{N}$  and  $V_{OO}$ . The data were collected from the lattices with  $N = 36, 64, 100$  and  $144$ , and the corresponding hole doping densities are  $0.167, 0.156, 0.140$  and  $0.152$ , respectively. For a fixed  $V_{OO}$ , the numerical results are fitted by the third polynomial function of  $1/\sqrt{N}$ . When  $V_{OO} = 0.0$  and  $-0.2$ , the fitted curves touch the horizontal axis at positive values, suggesting absence of long-range correlation between hole pairs in the thermodynamic limit ( $1/\sqrt{N} \rightarrow 0$ ). As  $V_{OO}$  is decreased to  $-0.4$ , the positive intersections with the vertical axis for both  $\bar{C}(R > 2.0)$  and  $\bar{V}(R > 2.0)$  clearly point towards the presence of long-range superconducting order in the thermodynamic limit. We would like to point out that the accuracy of extrapolation of our data to the thermodynamic limit is indeed affected by slightly different hole doping densities on different lattices, as well as limited lattice sizes accessible to CPMC simulations, nevertheless the monotonic increase of pairing correlation with decreasing  $V_{OO}$  strongly supports the

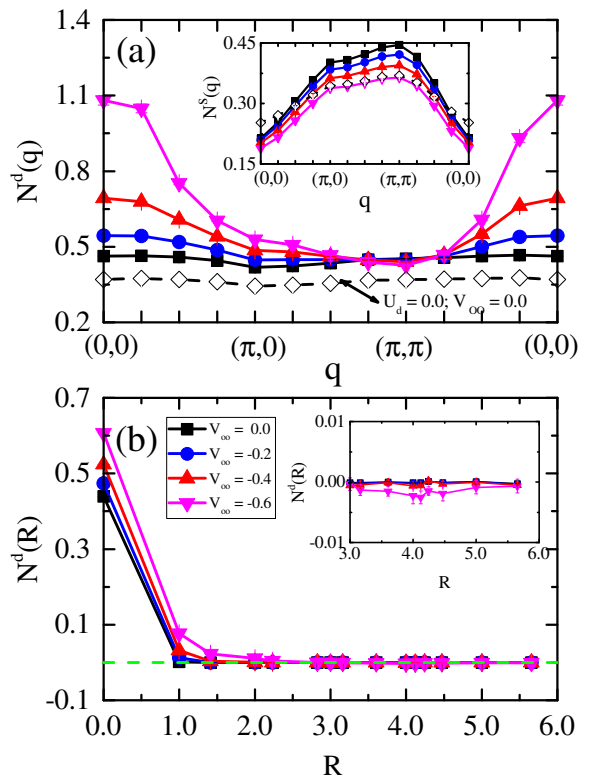


FIG. 3. (color online) (a) Nematic charge structure factor  $N^d(\mathbf{q})$  for different values of  $V_{OO}$  along the high symmetry lines in the first Brillouin zone. The open diamonds indicate the nematic charge structure factor of free-electron system. Inset: The charge structure factor  $N^s(\mathbf{q})$  with the s-wave form factor as a function of  $\mathbf{q}$ . (b) Nematic charge correlation  $N^d(R)$  for different values of  $V_{OO}$  as a function of the distance  $R$ . Inset: The enlarged nematic charge correlation for  $R \geq 3.0$ . The lattice size and hole doping density are the same as used in Fig. 1.

existence of d-wave SC beyond certain  $V_{OO}$ .

*Nematicity and CDW*– Next, we turn to discuss the effect of  $V_{OO}$  on the charge property. Fig. 3(a) displays  $N^d(\mathbf{q})$  as a function of wavevector  $\mathbf{q}$  and  $V_{OO}$  on the  $8 \times 8$  lattice at  $\delta = 0.156$ . At  $V_{OO} = 0.0$ , the shape of  $N^d(\mathbf{q})$  is very similar to the one of free-electron system ( $U_d = 0.0$ ), without obvious peak appearing in the curve. With decreasing  $V_{OO}$  from  $0.0$  to  $-0.6$ ,  $N^d(\mathbf{q})$  exhibits a monotonic increase at all  $\mathbf{q}$ 's except  $(\pi, \pi)$  and its nearby wavevectors, and this enhancement effect is particularly strong near  $\mathbf{q} = (0, 0)$ . The peak at  $\mathbf{q} = (0, 0)$  corresponds to a state in which the charge on the  $p^x$  orbital of each unit cell is larger than the one on the  $p^y$  orbital, or vice versa. This state is the so-called nematic phase. Meanwhile, the enhancement at nonzero  $\mathbf{q}$ 's signals the development of CDW with the d-wave form factor. It is worth noting that  $N^d(\mathbf{q})$  appearing at  $(\pi/2, 0)$  is consistent with the experimentally observed CDW peaked at  $([0.4\pi - 0.6\pi], 0)$  [15, 16], and stronger instability to charge ordering at  $\mathbf{q} = (0, 0)$  than at  $\mathbf{q} = (\pi/2, 0)$  naturally accounts for why nematicity sets in preceding the formation of CDW. As a comparison, we show

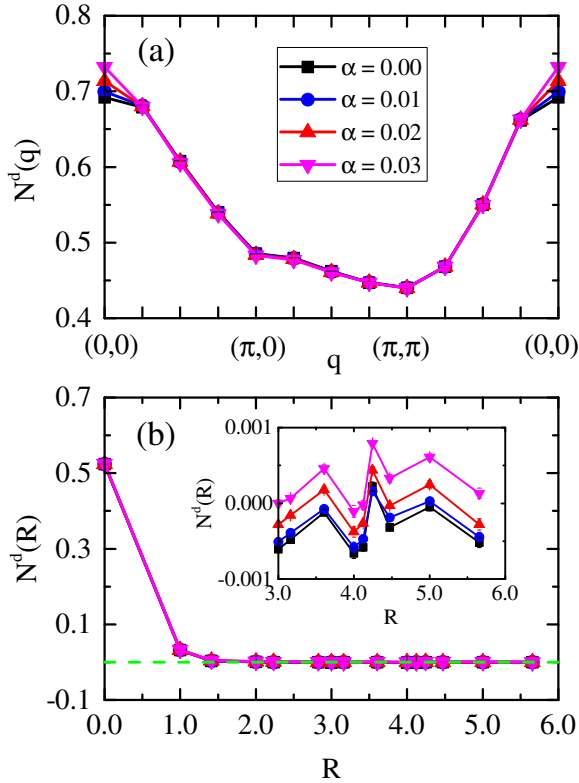


FIG. 4. (color online) (a) Nematic charge structure factor  $N^d(\mathbf{q})$  at  $V_{OO} = -0.4$  for different values of  $\alpha$  along the high symmetry lines in the first Brillouin zone. (b) Nematic charge correlation  $N^d(R)$  at  $V_{OO} = -0.4$  for different values of  $\alpha$  as a function of the distance  $R$ . Inset: The enlarged nematic charge correlation for  $R \geq 3.0$ . The lattice size and hole doping density are the same as used in Fig. 1.

in the inset of Fig. 3(a) the charge structure factor with the s-wave form factor,  $N^s(\mathbf{q})$ , obtained by replacing  $-$  with  $+$  in Eq. (6). One can readily see that decreasing  $V_{OO}$  leads to a suppression of  $N^s(\mathbf{q})$  at all  $\mathbf{q}'s$ , indicating that  $V_{OO}$  is not beneficial for the formation of CDW with the s-wave form factor.

Fig. 3(b) shows the nematic charge correlation  $N^d(R)$  as a function of  $R$  and  $V_{OO}$ . It is clear to see that only the short-range part of  $N^d(R)$  with  $R < 3.0$  is enhanced by  $V_{OO}$ , while the long-range part is close to zero and unaffected by  $V_{OO}$  within simulation accuracy, as shown in the inset figure. The rapid decrease of  $N^d(R)$  to vanishingly small values indicates that  $N^d(\mathbf{q})$  in Fig. 3(a) is contributed mainly from short-range nematic charge correlations and there is no long-range charge order in the studied model.

In high- $T_c$  cuprates, the  $C_4$  rotational symmetry of  $\text{CuO}_2$  plane can be broken by a transition from tetragonal to orthorhombic structure. To address the effect of symmetry breaking, we mimic the orthorhombic distortion by modifying the Cu-O hybridization as:  $|t_{pd}^{ij}| = (1 \pm \alpha)t_{pd}$ , where  $+$ ( $-$ ) applies if the Cu-O bond shrinks (stretches) by  $\alpha$ . Fig. 4 displays the  $\mathbf{q}$ -dependent  $N^d(\mathbf{q})$  and  $R$ -dependent  $N^d(R)$  for different  $\alpha$  on the  $8 \times 8$  lattice at  $\delta = 0.156$  and  $V_{OO} = -0.4$ .

We observe that increasing  $\alpha$  from 0.00 to 0.03 results in an enhancement of  $N^d(\mathbf{q})$  at  $\mathbf{q} = (0, 0)$ , but does not affect other ones at nonzero  $\mathbf{q}'s$ . The overlap of curves for different  $\alpha$  in Fig. 4(b) suggests that the change of  $N^d(R)$ , if exists, is much smaller than the scale of the vertical axis. As seen from the inset of Fig. 4(b), the orthorhombic distortion induces a weak but significant enhancement of long-range part of  $N^d(R)$ , which is crucial for the formation of long-range ordered nematic phase. Based on the results presented in Fig. 4, we can conclude that the orthorhombic distortion is important for nematicity, but has little effect on the CDW. On the other hand, almost  $\alpha$ -independent  $C(R)$  (not shown here) indicates that the d-wave SC is insensitive to the structure symmetry.

*Conclusion*– We have studied the superconducting and charge properties of high- $T_c$  cuprates within the extended three-band Emery model by using the CPMC method. The simulation results show that it is hard to establish the d-wave SC and charge order in the standard three-band Emery model. Upon turning on the attraction between oxygen orbitals, we observe a strong enhancement for both d-wave pairing correlation and nematic charge structure factor at zero and finite wavevectors, which leads to simultaneous development of d-wave SC, nematicity, and CDW. This finding provides a natural explanation for recent Raman scattering experiments, where it was found that the energy scales of d-wave SC, CDW, and pseudogap seem to be governed by a common microscopic interaction [22, 23]. We expect that finite temperature studies of the extended three-band Emery model will offer a deeper understanding of high- $T_c$  cuprates in the superconducting and pseudogap regions.

This work was supported by the National Natural Science Foundation of China (No. 11674087 and No. 11734002). We acknowledge partial support from NSAF U1930402.

\* huangzb@hubu.edu.cn

- [1] B. Keimer, S. A. Kivelson, M. R. Norman, S. Uchida, and J. Zaanen, *Nature* **518**, 179-186 (2015).
- [2] T. M. Rice, K.-Y. Yang, and F. C. Zhang, *Rep. Prog. Phys.* **75**, 016502 (2012).
- [3] M. Vojta, *Adv. Phys.* **58**, 699-820 (2009).
- [4] P. A. Lee, N. Nagaosa, and X.-G. Wen, *Rev. Mod. Phys.* **78**, 17-85 (2006).
- [5] A. Damascelli, Z. Hussain, Z.-X. Shen, *Rev. Mod. Phys.* **75**, 473-541 (2003).
- [6] C. M. Varma, *Phys. Rev. B* **99**, 224516 (2019).
- [7] P. A. Casey and P. W. Anderson, *Phys. Rev. Lett.* **106**, 097002 (2011).
- [8] C. W. Chu, L. Z. Deng, and B. Lv, *Physica C* **514**, 290-313 (2015).
- [9] Y. Ando, K. Segawa, S. Komiya, and A. N. Lavrov, *Phys. Rev. Lett.* **88**, 137005 (2002).
- [10] V. Hinkov, D. Haug, B. Fauqué, P. Bourges, Y. Sidis, A. Ivanov, C. Bernhard, C. T. Lin, and B. Keimer, *Science* **319**, 597-600 (2008).
- [11] Y. Sato, S. Kasahara, H. Murayama, Y. Kasahara, E.-G. Moon, T. Nishizaki, T. Loew, J. Porras, B. Keimer, T. Shibauchi, and



- Y. Matsuda, *Nat. Phys.* **13**, 1074-1078 (2017).
- [12] X. Li, C. Zou, Y. Ding, H. Yan, S. Ye, H. Li, Z. Hao, L. Zhao, X. Zhou, and Y. Wang, *Phys. Rev. X* **11**, 011007 (2021).
- [13] R. Daou, J. Chang, D. LeBoeuf, O. Cyr-Choinière, F. Laliberté, N. Doiron-Leyraud, B. J. Ramshaw, R.-X. Liang, D. A. Bonn, W. N. Hardy, and L. Taillefer, *Nature* **463**, 519-522 (2010).
- [14] M. J. Lawler, K. Fujita, J. Lee, A. R. Schmidt, Y. Kohsaka, C. K. Kim, H. Eisaki, S. Uchida, J. C. Davis, J. P. Sethna, and E.-A. Kim, *Nature* **466**, 347-351 (2010).
- [15] A. Frano, S. Blanco-Canosa, B. Keimer, and R. J. Birgeneau, *J. Phys.: Condens. Matter* **32**, 374005 (2020).
- [16] R. Comin and A. Damascelli, *Annu. Rev. Condens. Matter Phys.* **7**, 369-405 (2016).
- [17] X. M. Chen, V. Thampy, C. Mazzoli, A. M. Barbour, H. Miao, G. D. Gu, Y. Cao, J. M. Tranquada, M. P. M. Dean, and S. B. Wilkins, *Phys. Rev. Lett.* **117**, 167001 (2016).
- [18] S. Gerber, H. Jang, H. Nojiri, S. Matsuzawa, H. Yasumura, D. A. Bonn, R. Liang, W. N. Hardy, Z. Islam, A. Mehta, S. Song, M. Sikorski, D. Stefanescu, Y. Feng, S. A. Kivelson, T. P. Devereaux, Z.-X. Shen, C.-C. Kao, W.-S. Lee, D. Zhu, and J.-S. Lee, *Science* **350**, 949-952 (2015).
- [19] G. Ghiringhelli, M. Le Tacon, M. Minola, S. Blanco-Canosa, C. Mazzoli, N. B. Brookes, G. M. De Luca, A. Frano, D. G. Hawthorn, F. He, T. Loew, M. Moretti Sala, D. C. Peets, M. Salluzzo, E. Schierle, R. Sutarto, G. A. Sawatzky, E. Weschke, B. Keimer, and L. Braicovich, *Science* **337**, 821-825 (2012).
- [20] M. H. Hamidian, S. D. Edkins, C. K. Kim, J. C. Davis, A. P. Mackenzie, H. Eisaki, S. Uchida, M. J. Lawler, E.-A. Kim, S. Sachdev, and K. Fujita, *Nat. Phys.* **12**, 150-156 (2016).
- [21] R. Comin, R. Sutarto, F. He, E. H. da Silva Neto, L. Chauviere, A. Fraño, R. Liang, W. N. Hardy, D. A. Bonn, Y. Yoshida, H. Eisaki, A. J. Achkar, D. G. Hawthorn, B. Keimer, G. A. Sawatzky, and A. Damascelli, *Nat. Mater.* **14**, 796-800 (2015).
- [22] B. Loret, N. Auvray, Y. Gallais, M. Cazayous, A. Forget, D. Colson, M.-H. Julien, I. Paul, M. Civelli, and A. Sacuto, *Nat. Phys.* **15**, 771-775 (2019).
- [23] B. Loret, N. Auvray, G. D. Gu, A. Forget, D. Colson, M. Cazayous, Y. Gallais, I. Paul, M. Civelli, and A. Sacuto, *Phys. Rev. B* **101**, 214520 (2020).
- [24] H.-C. Jiang and T. P. Devereaux, *Science* **365**, 1424-1428 (2019).
- [25] K. Jiang, X. Wu, J. Hu, and Z. Wang, *Phys. Rev. Lett.* **121**, 227002 (2018).
- [26] S. Sakai, M. Civelli, and M. Imada, *Phys. Rev. Lett.* **116**, 057003 (2016).
- [27] P. Corboz, T. M. Rice, and M. Troyer, *Phys. Rev. Lett.* **113**, 046402 (2014).
- [28] E. Gull, O. Parcollet, and A. J. Millis, *Phys. Rev. Lett.* **110**, 216405 (2013).
- [29] S. Raghu, S. A. Kivelson, and D. J. Scalapino, *Phys. Rev. B* **81**, 224505 (2010).
- [30] B. M. Andersen, S. Graser, and P. J. Hirschfeld, *Phys. Rev. Lett.* **105**, 147002 (2010).
- [31] M. Capone and G. Kotliar, *Phys. Rev. B* **74**, 054513 (2006).
- [32] T. A. Maier, M. Jarrell, T. C. Schulthess, P. R. C. Kent, and J. B. White, *Phys. Rev. Lett.* **95**, 237001 (2005).
- [33] D. Sénéchal, P.-L. Lavertu, M.-A. Marois, and A.-M. S. Tremblay, *Phys. Rev. Lett.* **94**, 156404 (2005).
- [34] S. Sorella, G. B. Martins, F. Becca, C. Gazza, L. Capriotti, A. Parola, and E. Dagotto, *Phys. Rev. Lett.* **88**, 117002 (2002).
- [35] K. Kuroki and H. Aoki, *Phys. Rev. Lett.* **76**, 4400-4403 (1996).
- [36] M. Qin, C.-M. Chung, H. Shi, E. Vitali, C. Hubig, U. Schollwöck, S. R. White, and S. Zhang, *Phys. Rev. X* **10**, 031016 (2020).
- [37] A. S. Alexandrov and V. V. Kabanov, *Phys. Rev. Lett.* **106**, 136403 (2011).
- [38] T. Aimi and M. Imada, *J. Phys. Soc. Jpn.* **76**, 113708 (2007).
- [39] L. P. Pryadko, S. A. Kivelson, and O. Zachar, *Phys. Rev. Lett.* **92**, 067002 (2004).
- [40] C. T. Shih, Y. C. Chen, H. Q. Lin, and T. K. Lee, *Phys. Rev. Lett.* **81**, 1294-1297 (1998).
- [41] S. Zhang, J. Carlson, and J. E. Gubernatis, *Phys. Rev. Lett.* **78**, 4486-4489 (1997).
- [42] F. F. Assaad, W. Hanke, and D. J. Scalapino, *Phys. Rev. B* **50**, 12835-12850 (1994).
- [43] S. Slizovskiy, P. Rodriguez-Lopez, and J. J. Betouras, *Phys. Rev. B* **98**, 075126 (2018).
- [44] C. J. Halboth and W. Metzner, *Phys. Rev. Lett.* **85**, 5162-5165 (2000).
- [45] S. A. Kivelson, I. P. Bindloss, E. Fradkin, V. Oganesyan, J. M. Tranquada, A. Kapitulnik, and C. Howald, *Rev. Mod. Phys.* **75**, 1201 (2003).
- [46] S. A. Kivelson, E. Fradkin, and V. J. Emery, *Nature* **393**, 550-553 (1998).
- [47] X.-J. Zheng, Z.-B. Huang, and L.-J. Zou, *J. Phys. Soc. Jpn.* **83**, 024705 (2014).
- [48] S. Bulut, W. A. Atkinson, and A. P. Kampf, *Phys. Rev. B* **88**, 155132 (2013).
- [49] M. H. Fischer and E.-A. Kim, *Phys. Rev. B* **84**, 144502 (2011).
- [50] M. Zegrodnik, A. Biborski, and J. Spalek, *Eur. Phys. J. B* **93**, 183 (2020).
- [51] Y. Yamakawa and H. Kontani, *Phys. Rev. Lett.* **114**, 257001 (2015).
- [52] A. Thomson and S. Sachdev, *Phys. Rev. B* **91**, 115142 (2015).
- [53] V. J. Emery, *Phys. Rev. Lett.* **58**, 2794-2797 (1987).
- [54] Z. Chen, Y. Wang, S. N. Rebec, T. Jia, M. Hashimoto, D. Lu, B. Moritz, R. G. Moore, T. P. Devereaux, and Z.-X. Shen, *Science* **373**, 1235-1239 (2021).
- [55] B. P. P. Mallett, T. Wolf, E. Gilioli, F. Licci, G. V. M. Williams, A. B. Kaiser, N. W. Ashcroft, N. Suresh, and J. L. Tallon, *Phys. Rev. Lett.* **111**, 237001 (2013).
- [56] Y. Wang, Z. Chen, T. Shi, B. Moritz, Z.-X. Shen, and T. P. Devereaux, *arXiv:2107.05773*.
- [57] Z. B. Huang, H. Q. Lin, and E. Arrigoni, *Phys. Rev. B* **83**, 064521 (2011).
- [58] Z. B. Huang, W. Hanke, E. Arrigoni, and D. J. Scalapino, *Phys. Rev. B* **68**, 220507(R) (2003).
- [59] S. Zhang, J. Carlson, and J. E. Gubernatis, *Phys. Rev. Lett.* **74**, 3652-3655 (1995).
- [60] S. Zhang, J. Carlson, and J. E. Gubernatis, *Phys. Rev. B* **55**, 7464-7477 (1997).
- [61] M. Qin, H. Shi, and S. Zhang, *Phys. Rev. B* **94**, 235119 (2016).
- [62] M. Guerrero, J. E. Gubernatis, and S. Zhang, *Phys. Rev. B* **57**, 11980-11988 (1998).
- [63] Z. B. Huang, H. Q. Lin, and J. E. Gubernatis, *Phys. Rev. B* **63**, 115112 (2001).
- [64] S. R. White, D. J. Scalapino, R. L. Sugar, N. E. Bickers, and R. T. Scalettar, *Phys. Rev. B* **39**, R839-R842 (1989).
- [65] R. Micnas, J. Ranninger, and S. Robaszkiewicz, *Rev. Mod. Phys.* **62**, 113-171 (1990).
- [66] Z. B. Huang, H. Q. Lin, and J. E. Gubernatis, *Phys. Rev. B* **64**, 205101 (2001).
- [67] A. Nazarenko, A. Moreo, E. Dagotto, and J. Riera, *Phys. Rev. B* **54**, R768-R771 (1996).